Eur. Phys. J. E **24**, 317–324 (2007)
DOI 10.1140/epje/i2007-10242-0

THE EUROPEAN PHYSICAL JOURNAL E

Can deformation of a polymer film with a rigid coating model geophysical processes?

A.L. Volynskii[1,a] and S.L. Bazhenov[2,b]

[1] Faculty of Chemistry, Moscow State University, Leninskie gory, Moscow, 119992 Russia
[2] Institute of Synthetic Polymeric Materials, Russian Academy of Sciences, Profsoyuznaya ul. 70, Moscow, 117393 Russia

Received 5 March 2007 and Received in final form 20 September 2007
Published online: 20 December 2007 –

Abstract. The structural and mechanical behavior of polymer films with a thin rigid coating is analyzed. The behavior of such systems under applied stress is accompanied by the formation of a regular wavy surface relief and by regular fragmentation of the coating. The above phenomena are shown to be universal. Both phenomena (stress-induced development of a regular wavy surface relief and regular fragmentation of the coating) are provided by the specific features of mechanical stress transfer from a compliant soft support to a rigid thin coating. The above phenomena are associated with a specific structure of the system, which is referred to as "a rigid coating on a soft substratum" system (RCSS). Surface microrelief in RCSS systems is similar to the ocean floor relief in the vicinity of mid-oceanic ridges. Thus, the complex system composed of a young oceanic crust and upper Earth's mantle may be considered as typically "a solid coating on a soft substratum" system. Specific features of the ocean floor relief are analyzed in terms of the approach advanced for the description of the structural mechanical behavior of polymer films with a rigid coating. This analysis allowed to estimate the strength of an ocean floor.

PACS. 68.35.Gy Mechanical properties; surface strains – 91.55.Hj Folds and folding – 91.55.Jk Fractures and faults

1 Introduction

Recent years are characterized by an ever-growing interest in the systems composed of a thin rigid coating on a soft polymer substratum [1–6]. A special attention is focused on studying both the structural and mechanical aspects of their deformation. As was shown in [4–11], tensile drawing of such complex systems is accompanied by, at least, two general phenomena. First, tensile drawing entails the development of a regular wavy microrelief on the initially smooth surface [4–11]. Second, a rigid coating experiences its regular fragmentation (disintegration) on the bands of similar dimensions [1–4].

In the literature, the above complex systems are referred to as "*a rigid coating on a soft substratum*" systems. The specific conditions providing their unique behavior and fascinating properties were revealed. Theoretical expressions relating the parameters of the formed surface relief (period of regular microrelief and mean dimensions of fractured fragments) and mechanical properties of both coating and support were derived. The above relationships appear to be universal; hence, one may expect that they may be applied for the description of various "*a rigid coating on a soft substratum*" systems. Therefore, a polymer film coated with a thin rigid layer may be used as an accessible and simple model for the description of various natural events and phenomena.

In this work, the above approach is used for the description (modeling) of real natural phenomena.

2 Experimental

Commercial films based on amorphous unoriented poly(ethylene terephthalate) (PET), poly(vinyl chloride) (PVC), synthetic isoprene rubber (IR), and natural rubber (NR) were used as substrates. The thickness of PET and rubber films was equal to 100 and 500 μm, respectively. Rubber samples were crosslinked by 1.5 weight parts of dicumyl peroxide per 100 weight parts of raw rubber. Dumbbell-shaped specimens were cut from initial polymer films. The gage dimensions of the specimens were 6×22 mm. The surface of the test samples was decorated with a thin layer of gold or platinum (~ 15 nm) using the method of ionic-plasma sputtering. Then, the test samples were subjected to stretching on an Instron-1122 tensile machine. The strain rate was varied from 1 to

[a] e-mail: volynskii@mail.ru
[b] e-mail: Bazhenov@ispm.ru

500 mm/min; the stretching temperature was changed from room temperature to 105 °C.

For different substrates, different modes of loading were used. Decorated thermoplastic polymers (PET or PVC) were stretched at temperatures above their glass transition temperature T_g (75 °C for PET and 65 °C for PVC). At temperatures above T_g, polymers are soft, and their mechanical response is similar to that of rubbers. After stretching, the coated samples with fixed dimensions were cooled down to room temperature. This procedure prevents any contraction and strain recovery upon unloading.

The coated rubber samples were stretched at room temperature. To prevent any contraction of the deformed samples upon unloading, the samples were fixed by clamps.

To study the behavior of the composite samples in compression, initial uncoated rubber samples were stretched, and their dimensions were fixed; then, their surface was decorated with a platinum coating, and the coated samples were set free. Upon unloading, the stretched rubber samples fully restored their initial dimensions. This contraction entails the compression in the coating.

Surface of the test samples was studied by a Hitachi S-520 scanning electron microscope. The thickness of the deposited coating was estimated according to the following procedure: the platinum layer was deposited onto a smooth glass surface. Within fixed time intervals, the deposited coating was scratched, and the depth of the deposited layer was measured by the AFM method. As the layer thickness was proportional to the time of deposition, one could easily plot the calibration curve, and calculate the thickness of the deposited layer at a given exposure time.

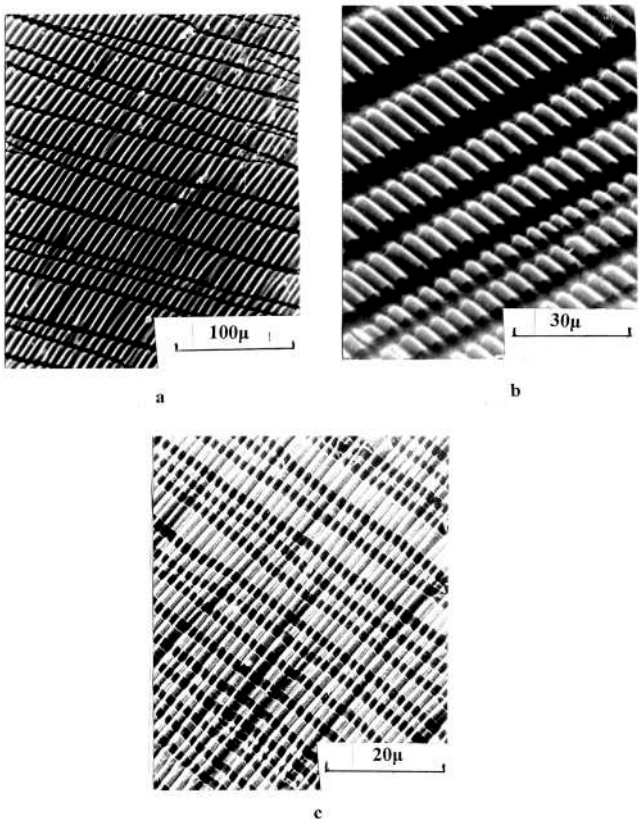

Fig. 1. SEM image of the NR sample with thin (15 nm) gold coating after its deformation at room temperature to tensile strain 50% (a); PVC sample with a thin (21 nm) platinum coating after its deformation at 90 °C to a tensile strain of 20% with a strain rate of 10 mm/min (b); and PET sample with a thin (15 nm) platinum coating after its deformation at 90 °C to a tensile strain of 100% with a strain rate of 1 mm/min (c).

3 Results and discussion

3.1 Development of a regular surface relief

Figures 1a–c present the SEM images for different coated polymer samples after their stretching. Dark and light bands are seen to be perpendicular to the direction of stretching. Dark bands correspond to cracks (grooves) in the coating, whereas light bands are the fragments of the fractured coating. Evidently, cracks in the coating are perpendicular to the direction of stretching. It is worth mentioning that two regular structures are formed on the surface of the deformed samples: a regular wavy relief and a uniform pattern of fractured fragments of a thin rigid coating. As follows from Figure 1, dark and light fragments are arranged into a regular wavy pattern. Both grooves and rises are oriented along the direction of tensile drawing. Even though quite different polymer substrates are used (NR is an elastic polymer, PVC is a ductile polymer, PET is a liquid-like polymer), the resultant surface pattern is practically identical.

According to [7], structures similar to those in Figure 1 may also be generated by using other loading conditions. For example, the polymer film is stretched, and the surface of the as-drawn film is coated with a thin rigid layer. When the test sample is unloaded, its length tends to recover its initial size. Figures 2a and b compare the corresponding microscopic images for the samples of synthetic rubber prepared in two different ways: by direct stretching of the coated sample and by contraction of the stretched sample with a thin rigid coating (the sample was coated after stretching).

In both cases, a regular surface relief is formed. The structure of this surface relief is *virtually* identical for both samples, and this fact suggests a common mechanism of their development. Despite a striking similarity between Figures 2a and b, there is an important difference between them. This difference concerns the orientation of microreliefs with respect to the tension direction. Microrelief produced by direct stretching of the test sample (Fig. 2a) is oriented along the drawing direction. However, microrelief induced by the contraction of the drawn sample is oriented perpendicular to the direction of tensile drawing (Fig. 2b). In our opinion, the orientation of relief is controlled by the *direction* of compression of a rigid coating, which stands behind the development of a wavy relief.

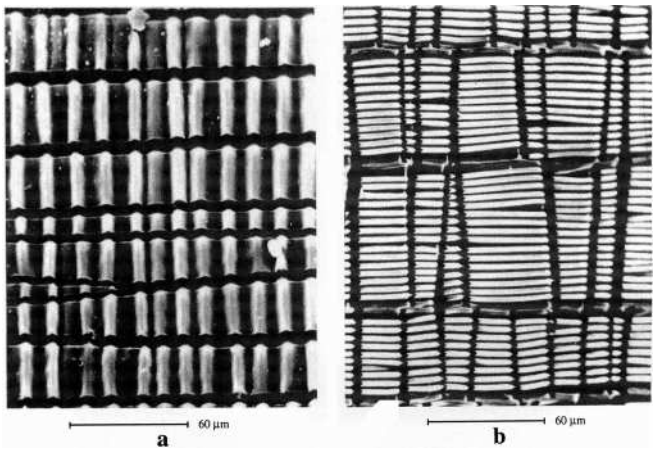

Fig. 2. SEM images of rubber samples coated with a thin (15 nm) platinum layer: (a) deformation is carried out for the Pt-coated sample to 50%; (b) initial rubber sample is drawn to a strain of 100%, the as-drawn sample was coated with Pt layer and allowed to shrink and recover its initial size. The axis of extension is vertical.

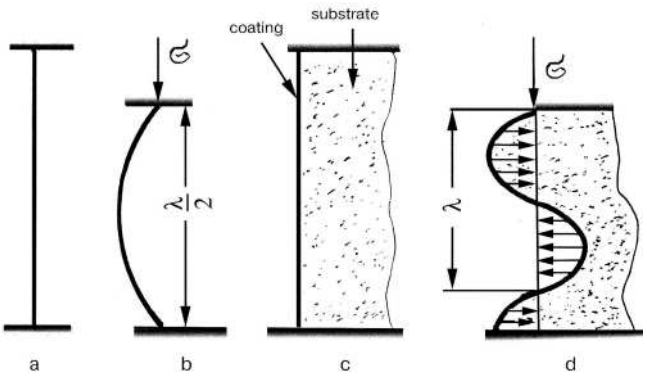

Fig. 3. Buckling instability for an anisodiametric body in a free state (a, b) and on a soft substratum (c, d).

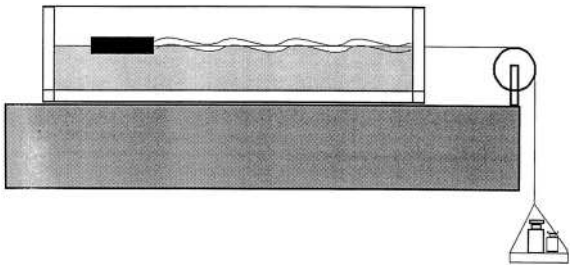

Fig. 4. Schematic representation of the equipment used for modeling of folding by Ramberg and Stephansson [18].

During tensile drawing, the volume of rubbery polymers remains virtually unchanged. Deformation is accompanied by a dramatic side contraction, which entails the contraction of the coating in the direction perpendicular to the direction of tensile drawing.

Upon contraction of the stretched sample, the direction of contraction coincides with the direction of the initial tensile drawing. In this case, microrelief is turned by 90° with respect to the direction of tensile drawing. As a result of contraction (shrinkage), microrelief is turned by 90° with respect to the microrelief produced by stretching. This experimental evidence makes it possible to arrive at the following conclusion. The development of surface microrelief is independent of the nature of stress (compressive or stretching stress) in the RCSS system. Compressive forces lead to the development of normally oriented tensile stress in the system, and vice versa, tensile stress generates normally directed compressive stress. In both cases, virtually identical structures are formed (Figs. 1 and 2). The only difference between them concerns the orientation of the formed surface structures relative to the direction of tensile drawing (compression).

The development of a regular microrelief is provided by the contraction of a rigid coating on a soft substratum. This conclusion concerning the key role of contraction in the development of the above microrelief seems to be very important. Let us consider the physical phenomena which take place during the compression of highly anisodiametric solids (in our experiments, a rigid coating). For the first time, such phenomena were considered by Euler more than 200 years ago. He showed that, under compression, an elastic rod buckles when a critical stress is attained. This rod acquires a sinusoidal shape with a wavelength which is equal to the doubled length of the compressed body (Figs. 3a and b) [6]. When a rod is firmly attached to a soft elastic substrate (Fig. 3c), the whole behavior under compression is changed. When the critical compression stress is attained, the rod is unable to acquire the half-wave shape (Fig. 3d) because, under its deviation from the linear direction, the restoring force from the support acts on the body, and this force is proportional to the value of deflection. As a result of this interaction between the external applied force and the induced internal resistance from the support, the coating will assume a sinusoidal shape with wavelength λ.

The problem of buckling under compression was first considered by Smoluchowski [11,12] at the beginning of the twentieth century. Later, this problem has been studied by Biot [13–15] and Ramberg [16,17]. They showed that a rigid coating bends under the action of compressive stresses. To reveal this mechanism controlling the formation of a regular surface relief, a method for the modeling of such processes was developed.

Seemingly, Ramberg was the first who proposed to model folding in rocks in terms of the structural and mechanical behavior of RCSS systems. Figure 4 presents the schematic representation of the experimental procedure advanced by Ramberg and Stephansson [18]. Stress is applied to an elastic coating (rubber or gelatin plate) floating on a dense but low-viscosity liquid (mercury, saturated solution of KI). Under such conditions, the authors reported the development of a regular wavy relief in a thin coating during its compression. Evidently, the modeling experiments by Ramberg and Stephansson [18] are able to illustrate folding in the coating but fail to describe cracking in the coating, which also takes place in the RCSS systems under their loading (including processes taking place in Nature).

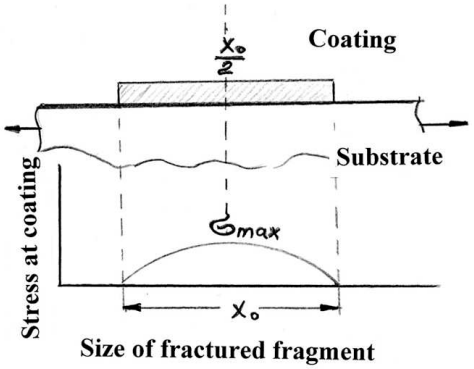

Fig. 5. Schematic drawing of a coating fragment adhered to a polymer substrate. The X-axis is chosen so that in the center of the fragment $x = 0$.

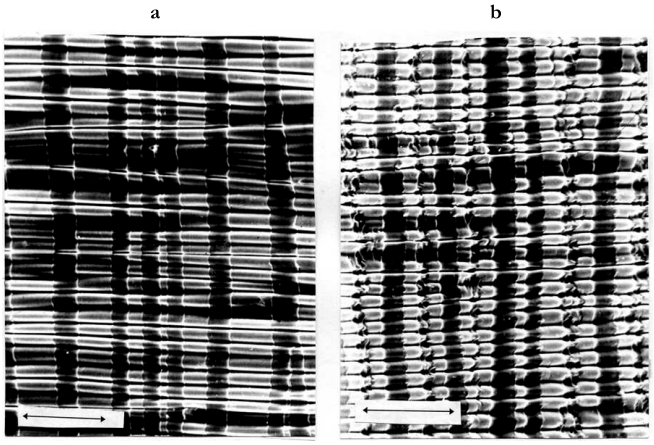

Fig. 6. (a) SEM micrograph of Pt/PET, elongated to 100% strain at a temperature of 100 °C. (b) Pt/PET elongated to a strain of 50% at 100 °C, and after that, elongated to a total strain of 100% at 85 °C. The cracks in the midlines of the fragment bands reveal the mechanism of fragmentation.

3.2 Regular fragmentation of coating

Now let us consider the process of a regular fragmentation (cracking) of the coating in more detail. As was shown in [4,6], a regular fragmentation of a rigid coating is provided by the specific features of the mechanical stress transfer from a soft substratum to a rigid coating through an interfacial boundary. The fracture of a rigid coating into numerous fragments of virtually similar dimensions may be explained as follows. At the early stages of stretching, the dimensions of fractured fragments are different. This is likely to be related to the fact that, at low strains, fragmentation in the coating is primarily provided by surface microdefects, which exist in any solid. Such defects serve as nucleation sites for cracks. Distribution of defects in the coating is random; hence fracture also shows a random and irregular character. However, the mechanism of further fracture or further disintegration of fractured fragments appears to be very interesting and unique. Figure 5 presents the schematic representation of stress distribution at each fractured fragment. Evidently, at the edges of the fractured fragment, the stress level is equal to zero. However, on moving away from the edges of the fractured fragment, the stress increases because the coating is firmly attached to the polymer support, where mechanical stress is still maintained. Hence, the maximum stress in the fractured fragment is achieved exactly at its center. Upon further tensile drawing, stress in the coating increases but the stress distribution profile remains unchanged; in other words, the whole stress epure is shifted to higher stresses while, at the edges of the fractured fragment, stress is still equal to zero. Finally, the stress at the center of the fractured fragment achieves the ultimate strength level, and this fragment breaks down into two fragments with equal dimensions. This mechanism of fracture via the breakdown of each fragment into two equal parts was first analytically analyzed in [3,6]. As was shown, the mean length (L) of the fractured fragments along the drawing axis is equal to

$$L = 4h(\sigma^*/\sigma_0), \qquad (1)$$

where h is the thickness of coating; σ^* is the ultimate strength of the coating, and σ_0 is the stress in the support. Experimental verification of equation (1) was performed in [6], and agreement of theoretical and experimental data is achieved.

Microscopic observations allowed one to obtain a direct evidence supporting the above mechanism of regular fracturing. Figure 6 shows the SEM images of the two samples of PET with a deposited platinum coating after their stretching by 100%. The first sample (Fig. 6a) was stretched at 100 °C to a tensile strain of 100%. As can be seen, the coating breaks down into fragments with a mean width of 3.5 μm. The second sample was stretched at 100 °C to a tensile strain of 50%; then, the temperature was decreased down to 80 °C, and the as-drawn sample was stretched at 80 °C by 100%. As a result of the above temperature drop, the stress at the support increases (from 0.7 to 3.5 MPa) and, as follows from Figure 6b, coating fragmentation recommences but, in this case, the mean sizes of the fractured fragments of the coating decrease down to 1.7 μm. The analysis of the mean dimensions of the newly formed fragments suggests that, as a result of the second loading cycle, almost each fragment of the fractured coating breaks down exactly into two equal parts. As is well seen, all fractured fragments break down strictly at their center. All the above features of the fracture of the metallic coating fully agree with the above speculations. Obviously, the fracture of a rigid coating is the only physical reason behind the regular arrangement of cracks in the coating or, in other words, behind the development of fractured fragments of similar dimensions.

3.3 Modeling natural process

We considered the most general properties of "a rigid coating on a soft substratum" (RCSS) systems. Such systems are very common in Nature (including fruit and bodies

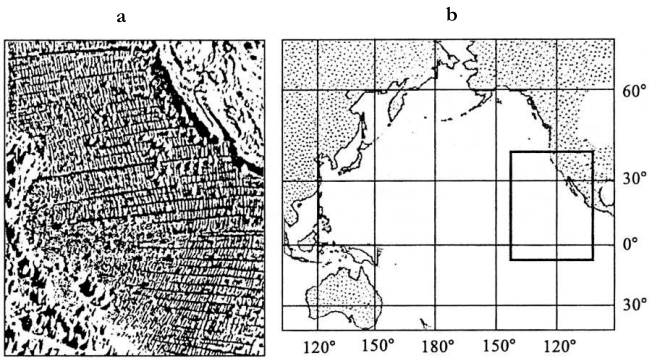

Fig. 7. Fragment of the ocean floor relief in the region of the middle ocean rise (a) and its location in the map of the Pacific Ocean (b).

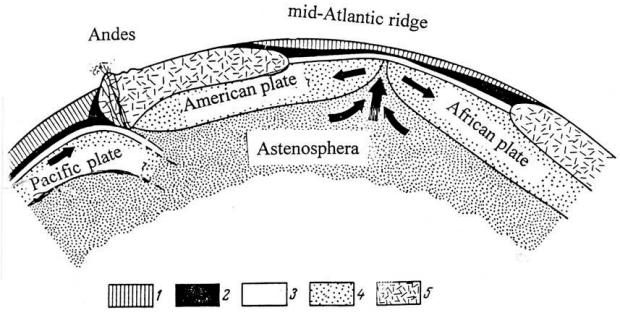

Fig. 8. Middle Atlantic ridge in terms of the tectonics of the lithospheric plates. 1: water; 2: sediment; 3: basaltic oceanic crust; 4: upper mantle; 5: continental crust.

of animals). In our opinion, our planet Earth presents a gigantic RCSS system. Striking morphological similarity between Earth's surface relief and microscopic relief induced in polymer films with a thin coating upon their stretching was described in [19]. Figures 7a and b present the maps of ocean floor relief in the northern and central parts of the Eastern Pacific Rising [20]. For comparison, Figure 1a shows the SEM image of the surface of a sample based on natural rubber and a thin (15 nm) gold layer after its stretching by 50%.

The morphological similarity between the presented patterns seems to be amazing. Cracks in the coating (Fig. 1a) are identical to the transform faults in the ocean crust. As is known, the system of transform faults is the most typical pattern of the ocean floor relief. Let us discuss two key features of this system. First, transform faults are always oriented almost perpendicular to the direction of mid-oceanic ridges and, hence, they are parallel to each other. Second, transform faults are located at almost equal distances from each other. Such arrangement implies that there are no somewhat appreciably long regions of the mid-oceanic ridges, which are free of transform faults. Therefore, one may unequivocally conclude that transform faults are involved in the characteristic structure of mid-oceanic ridges or, in other words, both structures present a unified system.

In our opinion, the morphological similarity between the microscopic surface relief of deformed polymer films with a rigid coating and the ocean floor relief [19] is understandable. This similarity may be explained as follows.

First, all modern concepts concerning Earth's structure allow one to model this body as "*a rigid coating on a soft substratum*" system. Indeed, a relatively thin (5–50 km) and rigid coating (lithosphere) rests on a relatively soft and mobile upper layer of the Earth's mantle (asthenosphere). A striking similarity between the RCSS systems with upper Earth's envelopes is also proved by the fact that the overall thickness of the Earth's mantle is equal to 2900 km, and this dimension is much higher than the thickness of the rigid crust.

Second, the principal tectonic stresses are assumed to be transferred from a viscous substance of the upper Earth's mantle to the lithosphere via convection. In other words, the principal stresses providing horizontal crust displacements, in particular drift of continents and development of relief via vertical displacements, show an evident endogenic genesis and act from the Earth's mantle. In this respect, one may conclude that this system is similar to the structure of deformed polymer films with a rigid coating.

Third, the analysis of the RCSS systems suggests that uniaxial compression of a rigid coating on a soft substratum inevitably leads to a uniaxial extension of the coating in the perpendicular direction, and vice versa [9]. In other words, it makes no difference which mode of deformation dominates: either uniaxial stretching or uniaxial compression. In the former case, tensile extension entails uniaxial compression of the coating in the perpendicular (relative to the direction of the tensile drawing axis) direction. In the latter case, uniaxial compression results in uniaxial stretching in the perpendicular (with respect to the axis of compression) direction. As was experimentally shown in the above-cited works, during uniaxial deformation of the RCSS systems, coating is *always* subjected to the action of both types of stresses: tensile stress and compressive stress, which is perpendicular to tensile stress. In our opinion, the latter observation is far from being trivial but presents an evident interest for modeling the development of the ocean floor relief.

Let us apply the approaches developed in [9–11] for modeling the development of the oceanic crust relief in the Atlantic mid-oceanic ridge. In this work, the development of the system of parallel cracks (transform faults) in the Earth's crust has been modeled and analyzed.

Let us consider the geodynamic situation in the region of the Atlantic mid-oceanic ridge in more detail. Figure 8 presents the section of the upper Earth's layers in this region, which is constructed on the basis of modern concepts concerning the tectonics of lithospheric plates. Let us note that a quite similar pattern is also typical of other mid-oceanic ridges because the geodynamic situations in these regions are virtually the same. According the above speculations, spreading of oceanic crust proceeds via the extrusion of the material of the upper Earth mantle (asthenosphere) through the mid-oceanic ridge [21]. Presently, broadening of the Atlantic Ocean takes place,

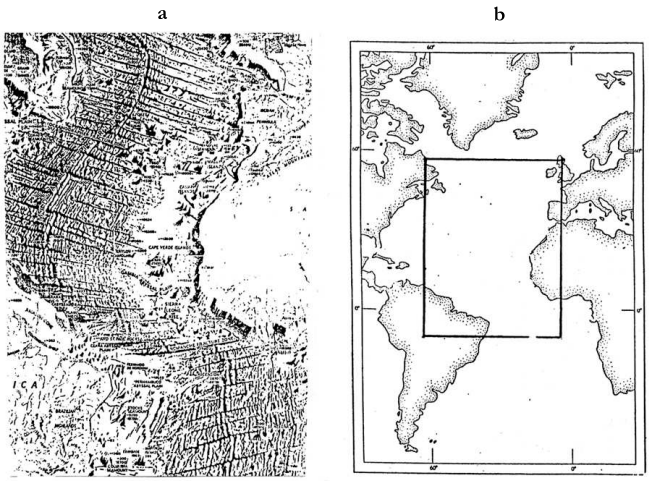

Fig. 9. Fragment of the ocean floor relief in the region of the middle Atlantic ridge (a) and its location on the map of the Atlantic Ocean (b).

and the American plate is drifted to the West with a speed of several centimeters per year. At the same time, the Pacific plate moves in the opposite direction under the American continent with the same speed (underthrusting). Evidently, as a result of this oncoming movement, all the American plate appears to be under the action of uniaxial compression. It is important to note that the compressive tectonic stress in the American plate is directed perpendicular to the direction of spreading (the axis of the mid-oceanic ridge). Note that experimental approaches developed by [9–11] and comparison of Figures 2a and b allow one to assume that the oceanic crust is compressed in the direction perpendicular to the direction of the Atlantic mid-oceanic ridge; as a result, it is extended in the direction parallel to the axis of the Atlantic mid-oceanic ridge.

Therefore, when a lithospheric plate is modeled as a fragment of the RCSS system, one should admit that its uniaxial deformation leads to the situation when a rigid coating is subjected to a simultaneous action of the two types of stresses: compression and tension. In other words, compressive stress acts in the direction perpendicular to the axis of the Atlantic mid-oceanic ridge, whereas the direction of tensile stress is parallel to this axis. Qualitatively, this observation allows one to understand why transform faults are always perpendicular to the axis of spreading. The point is that any crack always propagates in the direction perpendicular to the axis of the applied tensile stress. This statement is well illustrated by the maps of the ocean floor relief in the region of the Atlantic mid-oceanic ridge (Fig. 9) [20].

Within the framework of the advanced model, tensile stresses are assumed to act in the direction parallel to the axis of the mid-oceanic ridge. Another key assumption concerns the occurrence of multiple fracture events (cracking) in the coating during tensile drawing of a soft support (Fig. 9). This property of the RCSS systems has been derived and experimentally confirmed in [6,10]. Furthermore, the above approach allows one to determine the mean dimensions of the fractured fragments (distances between cracks in the coating) as a function of deformation conditions. This conclusion makes it possible to estimate the parameters of the ocean floor relief from direct measurements. Indeed, the analysis of the structural and mechanical behavior of the RCSS systems [6,10] leads to the following expression for the principal relief parameters:

$$L = 4h(\sigma^*/\sigma_0), \tag{1}$$

where L is the mean length of the fractured fragments along the drawing axis, h is the thickness of the coating; σ^* is the ultimate strength, and σ_0 is the stress in the substratum. In equation (1), L corresponds to the distance between transform faults, which may be directly estimated from the corresponding ocean floor maps. For the practical application of equation (1), one should necessarily know the relief-forming stress σ_0 in the undercrust layer of the upper Earth's mantle.

As is presently adopted, the driving force of spreading and, hence, drift of the continents is provided by a viscous convective flow of the material in the upper Earth's mantle (Fig. 8). To describe the process of a viscous flow, the most convenient way is offered by the Newtonian law, which allows one to calculate the stress maintaining the liquid flow (in other words, the stress in the mantle σ_0):

$$\sigma_0 = \eta \, \mathrm{d}\varepsilon/\mathrm{d}t, \tag{2}$$

where η is the viscosity, and $\mathrm{d}\varepsilon/\mathrm{d}t$ is the strain rate. Let us estimate this stress at $\eta = 10^{21}$ [22]. To this end, let us assume that the rate of the drift of continents is equal to the rate of viscous displacement of the material in the Earth's mantle adjacent to lithosphere. In this connection, the rate of flow of the material in the upper mantle is assumed to be equal to a reliably estimated rate of spreading (the drift rate of the continents). This rate or, in other words, strain rate in equation (2), is equal to

$$\mathrm{d}\varepsilon/\mathrm{d}t = (\Delta l/l_0)/\Delta t,$$

where l_0 is the initial distance between the continents, which is assumed to be equal to 5000 km; Δl is the displacement per year ($\Delta l = 10$ cm); Δt is the time (1 year) providing this displacement. By substituting the above estimates to equation (2), we arrive at $\sigma_0 \approx 0.6$ MPa, and this value corresponds to the relief-forming stress in the mantle. This estimate appears to be unexpectedly small. Note that this low stress may hardly be estimated for a real ocean crust. Usually, one may assess the stress level at stress-concentrating sites, for example, at subduction regions [23]. However, the primary source of such high local stresses may be perfectly provided by a low relic background stress (this value may be estimated through Eq. (2)) acting over rather long periods of time (possibly, during the whole period of spreading).

Nevertheless, the above-estimated value makes it possible to use equation (1) for the estimation of the strength of the Earth ocean crust. Hence, when the thickness of the Earth crust in the vicinity of the mid-oceanic ridge $h = 10$ km, the mean distance between the transform

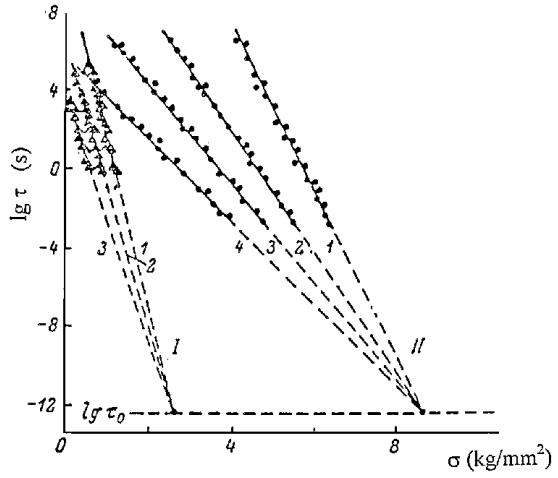

Fig. 10. Durability (lifetime) *vs.* tensile stress for (I) rock salt at 1) 400, 2) 500, and 3) 600 °C and (II) semicrystalline aluminum at 1) 18, 2) 100, 3) 200, and 4) 300 °C [18].

faults $L = 200$ km, and the tectonic stress $\sigma_0 \approx 0.6$ MPa, the strength of the Earth oceanic crust in the regions of transform faults is estimated to be equal to approximately 3 MPa. This value appears to be amazingly small. Therefore, the question arises as to whether the strength of the Earth oceanic crust is that small.

According to Griffith [24], the strength of a solid body is reversely proportional to the length of the largest crack in that body. The longer the defect the lower the strength of the body. In addition, the strength decreases with time. Athough the strength of solids is listed in many handbooks, this parameter may hardly be considered as one of their constants as, for example, melting temperature or specific heat capacity. Within the modern concepts concerning the strength of solids, fracture is treated as a certain thermofluctuation process, which is totally controlled by thermal oscillational molecular motion. In this connection, the fracture of solids presents a consecutive rupture of chemical bonds, which is primarily localized at the tip of a growing crack. In turn, the rupture of chemical bonds is controlled by thermal fluctuations taking place in any real solid. In this case, the mechanical stress just increases the probability of such fluctuation event, which leads to the rupture of chemical bonds in a solid. Taking into account the fact that the probability of the development of any fluctuation event is a function of time, fracture as a whole also is a function of time. As a result, the fracture of any solid is a function of time it is subjected to mechanical stress [24].

Figure 10 presents the stress-at-fracture (strength) plotted against the time of stress duration for the two different materials: rock salt (I) and semicrystalline aluminum (II) [24]. As can be seen, the strength of any solid, independently of its nature, is not a constant but is strongly controlled by the time of stress duration and temperature.

The thermofluctuation fracture of a solid may be described in terms of the Zhurkov equation:

$$\tau = \tau_0 \exp\left[(U_0 - \gamma\sigma)/RT\right], \qquad (3)$$

Table 1. Parameters of the Zhurkov equation [18].

	τ_0 (s)	U_0 (kCal/mol)	γ $\left(\frac{\text{kCal}\cdot\text{mm}^2}{\text{mol/kg}}\right)$
Metals	10^{-12}–10^{-13}	25–170	0.7–9.6
Ionic crystals	10^{-12}–10^{-13}	31–74	14–60
Covalent bonds	10^{-12}–10^{-13}	91–113	–
Glasses	10^{-12}–10^{-13}	45–90	–
Polymers	10^{-12}–10^{-13}	25–53	0.14–0.9

where τ is the time up to fracture, U_0 is the activation energy of the fracture (rupture of chemical bonds in the solid), γ is the so-called activation volume where an elementary fracture event takes place (rupture of chemical bonds). In this case, τ_0 stands for the frequency of thermal vibrations of individual atoms in a solid relative to their equilibrium positions; σ is the applied constant stress; R is the universal gas constant, and T is the absolute temperature. Let us mention that the experimental data presented in Figure 10 allow one to assess all parameters of the Zhurkov equation.

To apply the Zhurkov equation for the estimation of the Earth's crust strength, one should model the oceanic crust as an integral solid. In our opinion, the analysis of the patterns developed upon the deformation of the RCSS systems and the comparison of such patterns with the maps of the ocean floor relief allow one to consider the Earth's crust as an independent physical gigantic object and as an integral solid. This solid is characterized by a spherical shape, variable chemical composition, and by thickness, temperature and density gradient, defectness, and many other parameters. Nevertheless, this is an integral anisodiametric solid relying on a soft support. This approach to modeling the Earth as an integral solid, which is able to accept and transfer the mechanical stresses over rather long distances (within oceans and my be in a global scale), allows one to apply the concepts on the RCSS systems for modeling the processes taking place in the oceanic crust. This method makes it possible to assess the level and direction of the acting stresses in the undercrust layer and strength. Evidently, the strength of a basalt fragment, which may be easily estimated in trivial experiments, is quite different from the strength of the Earth's crust as a whole. Obviously, it seems quite impossible to estimate the above characteristics for the Earth's crust as an integral solid by any other method.

The above approach offers two unique advantages. First, it allows an unprecedented opportunity to assess the stress-strain properties of such a colossal solid as the Earth's crust. Second, so far, the strength of solids was estimated under the action of a constant load during relatively short periods of time as hours or days (Fig. 10). For processes taking place in the oceanic crust, the time of stress duration spans over millions of years.

In this case, the principal problem concerns the estimation of the parameters of the Zhurkov equation for such a complex solid as oceanic crust. Table 1 lists the

experimental estimates of the parameters of the Zhurkov equation for various solids. As is seen, the parameter τ_0 remains almost unchanged for various solids. This result seems to be quite expected because the frequency of thermal oscillations in a solid is almost independent of its nature. The parameter U_0 is equal to several dozens of kCal/mol, and this corresponds to the energy of rupture of various intermolecular bonds.

Presently, the physical meaning of the parameters given in Table 1 for such a complex subject as the Earth's crust is still vague. Therefore, let us invoke the mean values of the parameters in the Zhurkov equation. For rough estimates of the mechanical durability (lifetime) of the Earth's crust, let us assume, for simplicity, that $\tau_0 = 10^{-12}$ s, $U_0 = 50$ kCal/mol, $\gamma = 1$ (kCal $\cdot$ mm^2/mol $\cdot$ kg), $R = 0.002$ kCal/mol K, $T = 400$ K, $\sigma = 0.2$ kg/mm^2. By substituting the above-estimated values to equation (3), we arrive at the conclusion that the time to fracture of the Earth's crust at such a low stress level is equal to about $\sim 3.0 \times 10^7$ (30 millions) years.

Of course, this estimate is very approximate because this approach requires the application of far more accurate data to the thickness of the Earth's crust, temperature, and other factors. The objective of this work is to demonstrate the potential and feasibility of this approach for modeling geodynamic processes. This finding might appear to be useful because, presently, one may estimate the age of rocks but the period of development of the various morphological forms of the Earth surface still remains an open problem.

We would like to thank Profs. V.E. Khain, N.V. Koronovsky, M.A. Goncharov, and Dr. O.V. Arzhakova for stimulating discussions. We acknowledge the financial support from the Russian Foundation for Basic Research (project Nos. 05-03-32538 and 06-03-32452).

References

1. D.R. Wheeler, H. Osaki, ACS Symp. Ser. **440**, 500 (1990).
2. T. Horniq, I.M. Sokolov, A. Blumen, A. Phys. Rev. E **54**, 4293 (1996).
3. Y. Leterrier, L. Boogh, J. Andersons, J.-A.E. Manson, J. Polym. Sci. Part B: Polym. Phys. **35**, 1449 (1997).
4. S.L. Bazhenov, I.V. Chernov, A.L. Volynskii, N.F. Bakeev, Dokl. Acad. Nauk **356**, 199 (1997).
5. N. Bowden, S. Brittain, A.G. Evans, J.W. Hutchinson, G.M. Whitesides, Nature **393**, 146 (1998).
6. A.L. Volynskii, S. Bazhenov, O.V. Lebedeva, A.N. Ozerin, N.F. Bakeev, J. Appl. Polym. Sci. **72**, 1267 (1999).
7. N. Bowden, W.T.S. Huck, K.E. Paul, G.M. Whiteside, Appl. Phys. Lett. **75**, 2557 (1999).
8. W.T.S. Huck, N. Bowden, P. Onck, T. Pardoen, J.W. Hutchinson, G.M. Whiteside, Langmuir **16**, 3497 (2000).
9. A.L. Volynskii, S.L. Bazhenov, O.V. Lebedeva, N.F. Bakeev, J. Mater. Sci. **35**, 547 (2000).
10. S.L. Bazhenov, A.L. Volynskii, V.M. Alexandrov, N.F. Bakeev, J. Polym. Sci. Part B: Polym. Phys. **40**, 10 (2002).
11. M. Smoluchowskii, Abh. Akad. Wiss. Krakau, Math. **K1**, 3 (1909).
12. M. Smoluchowskii, Abh. Akad. Wiss. Krakau, Math. **K1**, 727 (1910).
13. M.A. Biot, J. Appl. Phys. **25**, 2133 (1954).
14. M.A. Biot, Q. Appl. Math. **17**, 722 (1959).
15. M.A. Biot, *Mechanics of Incremental Deformations* (Wiley, New York, 1965).
16. H. Ramberg, Bull. Am. Assoc. Petrol. Geologists **47**, 484 (1963).
17. H. Ramberg, Tectonophysics **9**, 307 (1964).
18. H. Ramberg, O. Stephansson, Tectonophysics **1**, 101 (1964).
19. A.L. Volynskii, S.L. Bazhenov, Geofis. Int. **40**, 87 (2001).
20. B.C. Heezen, M. Tharp, *World Ocean Floor* (Office of Naval Research, US Navy, 1977).
21. P.R. Shaw, Nature **358**, 490 (1992).
22. L.M. Cathes, *The Viscosity of the Earth Mantle* (Princeton University Press, New York, 1975).
23. M.L. Zoback, M.D. Zoback, J. Adams, M. Assumpcao, S. Bell, E.A. Bergman, P. Blumbereg, N.R. Brereton, D. Denham, J. Ding, K. Fuchs, N. Gay, S. Gregersen, H.K. Gupta, A. Gvishiani, K. Jacob, R. Klein, P. Knoll, M. Magee, J.L. Mercier, B.C. Muller, C. Paquin, K. Rajendran, O. Stephansson, G. Suarez, M. Suter, A. Udias, Z.H. Xu, M. Zhizhin, Nature **341**, 291 (1989).
24. V.R. Regel, A.I. Slutsker, E.E. Tomashevskii, *Kinetic Nature of Strength in Solids* (Nauka, Moscow, 1974).
25. A.A. Griffith, *Theory of Rupture*, in *Proceedings of the 1st International Conference on Applied Mechanics, Delft, Holland (1924)* p. 55.